

# A Silicon Detector System on Carbon Fiber Support at Small Radius

Marvin Johnson

**Abstract**—The design of a silicon detector for a  $\bar{p}p$  collider experiment will be described. The detector uses a carbon fiber support structure with sensors positioned at small radius with respect to the beam. A brief overview of the mechanical design is given. The emphasis is on the electrical characteristics of the detector. General principles involved in grounding systems with carbon fiber structures will be covered. The electrical characteristics of the carbon fiber support structure will be presented. Test results imply that carbon fiber must be regarded as a conductor for the frequency region of interest of 10 to 100 MHz. No distinction is found between carbon fiber and copper. Performance results on noise due to pick-up through the low mass fine pitch cables carrying the analogue signals and floating metal is discussed.

**Index Terms**— Carbon Fiber, Silicon.

## I. INTRODUCTION

Carbon Fiber support structures have become common elements of silicon vertex detector designs. Because of mass, radiation damage and cooling considerations the sensors for the innermost layer of silicon detectors for  $\bar{p}p$  collider detectors are often mounted on a carbon fiber support structure. An example of such a detector is the Layer 00 detector for the CDF collaboration at the Fermilab Tevatron collider. While the use of carbon fiber solves a variety of mechanical problems, it presents a challenging set of electrical concerns. Highly conductive carbon fiber surfaces can capacitively couple noise into sensors, electronics and cables. The performance of the CDF Layer 00 detector is compromised due to significant coherent noise pickup [1]. Well-designed coupling and grounding schemes are essential for producing low-noise environments within the detectors. Here we describe the design of an inner layer silicon tracker that has been proposed for the Dzero experiment at the Fermilab Tevatron collider [2]. The design addresses all potential noise sources. A grounding scheme is proposed that minimizes noise pickup and retains an adequate signal to noise ratio.

The support structure for the proposed silicon detector consists of a twelve-sided inner shell and a six-sided outer shell. The inner shell has a 4-layer  $[0^\circ/90^\circ]_s$  lay-up of K13C2U high modulus carbon fiber. The outer shell has a 6-layer  $[0^\circ/+20^\circ/-20^\circ]_s$  lay-up of the same high modulus carbon fiber. This structure extends from  $Z=-380$  to  $Z=+380$  mm. A 0.025 mm kapton sheet with an embedded copper mesh is co-bonded to the outer shell for grounding connections.

The silicon sensors are mounted on the outer shell using epoxy adhesive. A low-pass filter for the bias high voltage is glued onto the sensor close to the wire bonding pads. It consists

of a 1210 3.9 nF capacitor, and a 0603 10k  $\Omega$  resistor. They are placed on top of a G-10 substrate with a thickness of 200  $\mu\text{m}$ . Both the high voltage and the ground on the filter card are provided through an analogue cable (see below).

## II. CARBON FIBER SUPPORT STRUCTURE

Highly conductive carbon fiber used for the mechanical support structure has the potential to exhibit strong capacitive coupling to the sensors. It is imperative that all the carbon fiber in the detector is effectively shorted to the hybrid or bias filter grounds to prevent capacitive noise transmission to the sensor readout. A series of tests were carried out to verify the conductivity of carbon fiber.

Two identically sized parallel plate capacitors (15 cm on a side) were constructed: the first with one copper plate and one type K139 carbon fiber plate; the second with two copper plates. A network analyzer was connected across this capacitor with one lead soldered to the copper plate and the other taped to the carbon fiber with copper tape. Increasing the area of copper tape on the carbon fiber plate dramatically increased the value of the capacitance up to a saturation point of about 25  $\text{cm}^2$  (a little over 10% of the area). At this point the capacitance of the carbon fiber - copper capacitor was identical to the capacitor with both plates made of copper ( $132 \pm 2$  pF). It should be noted that K13C is even more conductive than K139.

A test was also conducted to determine the feasibility of shorting a prototype K13C carbon fiber support cylinder to a hybrid or filter ground plane. The interior of the castellated support structure was driven with the source power from the network analyzer. A sensor/filter mockup constructed of aluminum and Kapton layers was mounted on the cylinder. The network analyzer input was wired to the sensor aluminum layer and both the source and input grounds were connected to the filter plane. Transfer functions to the sensor were measured with different configurations for shorting the carbon fiber to the filter plane. One to four  $\frac{1}{8}$ " wide strips of 1  $\mu\text{m}$  thick aluminized Mylar, 0.5 mil aluminum, or copper tape were attached between the filter and the carbon fiber. The effectiveness of the grounding strips was tested with and without additional copper tape coupling the network analyzer source to the carbon fiber. The aluminized Mylar strips were minimally effective in reducing power to the sensor. Aluminum and copper strips performed equally well. The power reduction was independent of the number of strips, but proportional to the amount of copper tape used to couple the strips to the carbon fiber. We

achieved a maximum reduction of 40 dB at 1 MHz with copper tape covering about 10% of the carbon fiber.

Because copper tape coupling would not be feasible in the detector, a coupling test was carried out using carbon fiber pieces with embedded aluminum foil and aluminized Mylar. The aluminum or Mylar was attached to the carbon fiber by co-curing it with the carbon fiber. A new sensor/hybrid mockup was built and mounted on different pieces of K13C carbon fiber which had various amounts of surface area covered with embedded aluminum. The embedded aluminum extends out to grounding strips that fold over and attach to the hybrid/filter plane (see also Fig. 1). The coupling point on the actual planes will be 2 mm wide ground pads. Aluminized Mylar grounding produced significantly less attenuation than aluminum; about 10 dB less below 20 MHz. This test also verified that the attenuation is not affected by the width of the grounding strips. Measurements of transfer functions were taken with different areas of embedded aluminum and equal sized grounding strips. Those data confirmed that the attenuation increases with contact area to the carbon fiber. The maximum area of embedded aluminum tested was 4 in<sup>2</sup> (again, about 10% of the area), giving a power decrease of at least 30 dB for all frequencies below 50 MHz. Coupling to carbon fiber through embedded aluminum has thus been shown to be an effective grounding technique. These studies have led to the design described in the next section.

### III. EXPERIMENTAL SETUP

For these tests, a carbon fiber support structure of K13C2U high modulus carbon fiber was used with embedded Kapton-copper mesh (co-cured with the carbon fiber). The back plane of the sensors mounted on the support structure were separated from the Kapton mesh by an insulating two-layer Kapton flex circuit. The flex circuit has one tab on either side that wraps around the sensor and is attached to the filter card mounted on the sensor. One of the insulating Kapton layers, which has a copper mesh circuit with vias, is connected to the copper mesh that is co-bonded in the outer shell of the support structure. The tab is folded around the sensor and attached to the ground on the filter card. The second layer takes the high voltage from the filter card and directly applies the bias voltage through the flex circuit to the backside of the sensor. Figure 1 shows a schematic cross section of the design.

Due to space constraints and heat dissipation, the signals from the silicon sensors are transmitted to the hybrid containing the SVX4 chips by flexible circuits up to 435 mm long. Since these circuits carry analogue signals they are dubbed analogue cables. This solution is very attractive because of reduced material and heat generation in the sensitive volume. However, this approach represents a considerable technical challenge. The addition of the analog cable reduces the signal to noise of the silicon sensors. Procurement of the flex cables and the complicated ladder assembly are other non-trivial issues. Moreover, noise pick-up could make the detector inoperable. One of the most important aspects in the design and technical

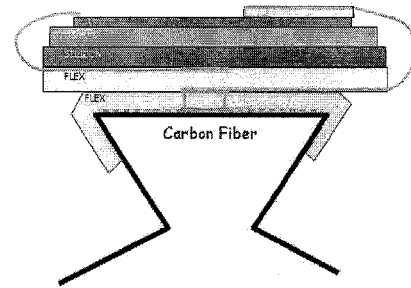


Fig. 1. Schematic cross section of the electrical configuration.

realization of a long analog cable is the capacitance between the traces, which has to be as small as possible.

To optimize the S/N ratio, our design uses a stack of two cables with constant 91  $\mu\text{m}$  pitch, laminated with a lateral shift of 45  $\mu\text{m}$ . In order to reduce the capacitance contribution from the adjacent cables, a spacer consisting of 150-200  $\mu\text{m}$  thick polypropylene mesh with about 25% volume occupancy is placed between the two cables. After a series of prototyping, flawless cables were produced by Dyconex [3]. The capacitance as measured for this arrangement is 0.36 pF/cm in good agreement with ANSYS calculations. In our setup we used 42 cm long prototype cables. Each cable has 129 (one for spare) 91  $\mu\text{m}$  pitch signal traces with a width of 16  $\mu\text{m}$  on a 50  $\mu\text{m}$  thick Kapton substrate. It also has two wider (100  $\mu\text{m}$ ) traces for HV and its return.

The analogue cable is wirebonded to a ceramic hybrid containing two SVX4 readout chips with 128 input channels each. The SVX4 chips amplify and digitize the signals and transmit them to a digital jumper cable through a 50-pin AVX connector.

The whole silicon sensor module was placed on copper-clad G10 with 70  $\mu\text{m}$  thick Kapton tape for insulation. The surface, i.e. the copper, of the copper-clad G10 was connected to the ground of the readout system and the High Voltage power supply. The whole assembly was put inside a dark box made of plastic. The noise was measured with this configuration. The results are presented in the next section.

After the above measurements, the sensor was placed on the carbon fiber support structure. The p-side of the sensor was grounded to the carbon fiber support structure through the biasing R-C filter on the sensor and the embedded copper clad Kapton flex circuit. It was attached with grounding tabs as described above. The Kapton flex was co-cured with the carbon fiber support so that it is an integral part of the support structure. The hybrid with the ceramic underneath was glued on top of the carbon fiber extension to the support structure. A photograph of the L0 module on the support structure plus

its extension is displayed in Fig. 2. Note that the carbon fiber

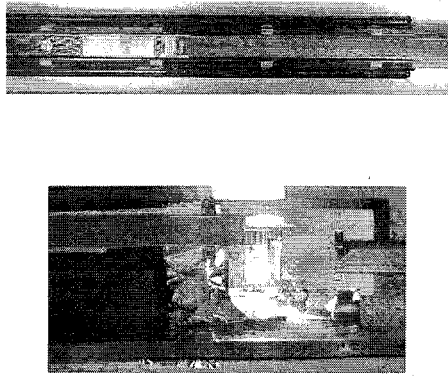


Fig. 2. Photograph showing a detail of the sensor part of the assembly installed on the L0 support structure (top); Photograph showing the hybrid part installed on the carbon fiber extension (bottom).

extension was electrically not well connected to the L0 support structure. Also, the DC resistance of the 47 cm long device was  $12\ \Omega$ . This assembly was mounted inside an aluminum Faraday cage. The Faraday cage was placed on the copper-clad G10 described above. Again the copper-clad G10 was connected to the ground of the readout system and the HV power supply. The electrical connection between the copper-clad G10 and the Faraday cage was quite good; the resistance was measured to be less than  $1\ \Omega$ .

#### IV. TEST RESULTS

First, we describe the test results for the L0 module before installing it on the prototype support structure. This result serves as a reference for the effect of adding the support structure. Next, we present the test results for several different grounding configurations after the installation.

##### A. Before Installation

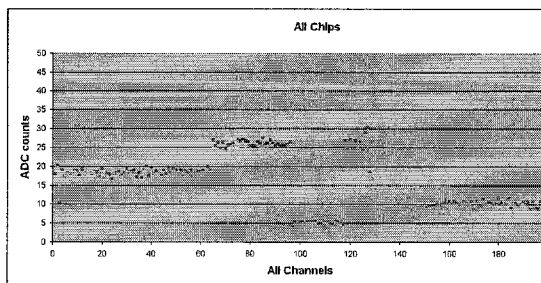


Fig. 3. Total (red squares) and differential (light blue circles) noise for the L0 module before installation onto the support structure as function of channel number. The units are  $\times 10$  ADC counts.

Figure 3 shows the total noise and differential noise for each readout channel. The first half of the chip, the first 64 channels, are connected to the analog cable only. The second

half is connected to both the analog cable and the sensor. The noise of a few channels in another 'bare' chip, is also shown for reference. The bandwidth setting of the SVX4 was fixed to four in our testing<sup>1</sup>. The resulting risetime is fast enough not to change the gain ( $<10\%$ ) even though the capacitive load changes within our region of interest<sup>2</sup>. We simply quote the ADC count as a unit representing the size of noise for the following comparisons with different grounding schemes or test setup configurations.

##### B. After Installation

As shown in Fig. 3, the total noise before installation was 2.7 ADC counts for channels connected to both the sensor and the analog cable. After installing the module onto the L0 support structure as described in Section III, the noise level went up to more than 50 ADC counts, indicating the need for additional grounding. We tested the following three grounding schemes.

- A Hybrid Ground. One end of a thin wire is soldered to the ground on the hybrid. The other end is taped to the Faraday cage by copper tape.
- B Sensor Ground. As described in Section III, the sensor is grounded to the L0 support structure. We connected the support structure to the Faraday cage with copper tape. One end was taped to the chassis of the Faraday cage, and the other end to the gold pads on the Kapton flex embedded onto the support structure.
- C Both Hybrid Ground and Sensor Ground.

Each grounding scheme gives a noise level of  $\sim 4.8$  (A),  $\sim 70$  (B), and  $\sim 10$  (C) ADC counts, respectively. The noise distributions are shown in Fig. 4. Because the ground trace on the analog cable has a resistance of about  $20\ \Omega$ , the actual signal return is the chassis of the Faraday cage for methods (B) and (C), as shown in the top of Fig. 5.

We observed that the Sensor Ground has the largest and the Hybrid Ground has the smallest ground loop so the observations above imply that the noise level is affected by the size of ground loop.

In order to minimize the area of the ground loop we placed a Kapton flex circuit under the analog cable and on top of the extension for supporting the hybrid. One end was attached to the gold pad on the Kapton flex circuit that was co-cured onto the L0 support structure. The other end was connected to the hybrid by a thin wire. The equivalent circuit diagram is shown in the bottom of Fig. 5. The resulting noise distribution for (C) is shown in Fig. 6. The noise level was reduced from the original value of 10 ADC counts to  $\sim 3.8$  ADC counts.

High impedance ground connections can cause a potential difference between the reference point of the hybrid (or actually the preamp in the SVX4) and the sensor, resulting in noise.

<sup>1</sup>The 10-90% risetime is measured to be 35 ns and 65 ns for 10 pF and 33 pF capacitive load, respectively. On the other hand, the integration time of the preamp is 132 ns.

<sup>2</sup>The SVX4 chip has a noise of 700 electrons per ADC count for the parameter settings used for our tests.

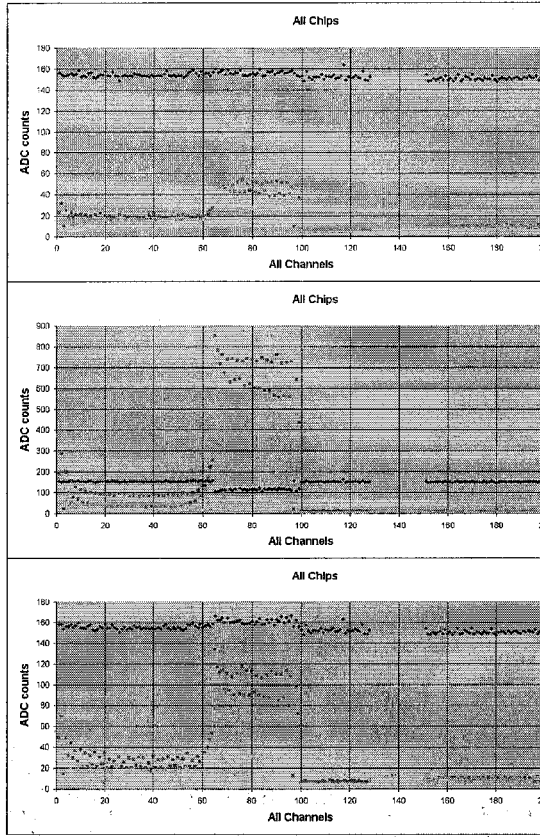


Fig. 4. Noise distribution after installing the L0 module onto the support structure. The top, middle, and bottom figures show the distributions corresponding to grounding scheme (A), (B), and (C), respectively. The total noise is represented by red squares, the differential noise by light blue circles, and the pedestal by the black diamonds. The units are ADC counts for the pedestal and  $\times 10$  ADC counts for the noise.

Therefore, a low impedance ground connection is crucial for minimum noise. Both resistance and inductance contribute to the impedance but for high frequencies, the inductance often dominates. For the L0 system a low impedance connection is equivalent to a low inductance connection. The impact of inductance in the ground connection is shown in Fig. 7 which shows the total noise as a function of the number of wires used for grounding scheme (C). For this test we have removed the extra Kapton flex ground connection between the support structure and the carbon fiber support structure. The wire length is about 4 cm each. Because the resistance of each wire is quite small, much less than the other connections in the ground path, this dependence is due to the inductance of the wires. Shortening the wire length from 4 cm to  $\sim 1.5$  cm suppresses the noise by  $\sim 10\%$ . Adding the extra ground connection and replacing the ground wire with two short ones reduces the noise of the Hybrid Ground from 4.8 to less than 3 ADC counts.

To summarize the test results, there are two key requirements for low noise in L0; *i*) The ground loop must be minimized, and *ii*) there must be a low impedance ground connection between the sensor and the SVX4 chip.

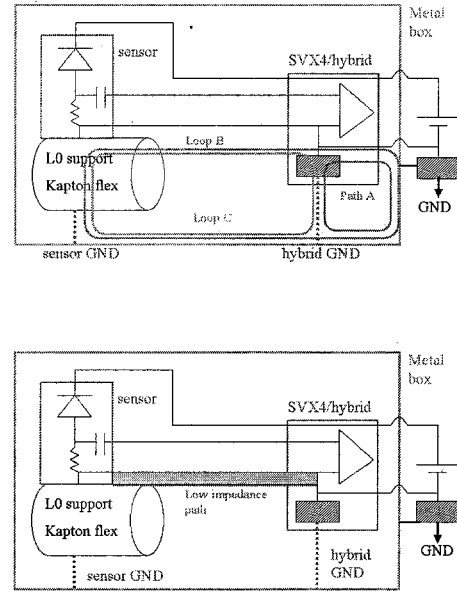


Fig. 5. The equivalent circuit diagrams for the test setups; see text for details.

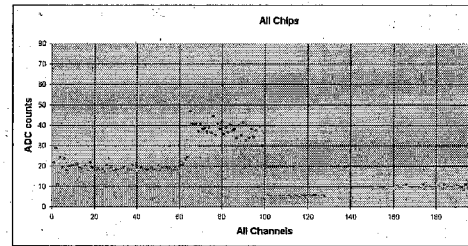


Fig. 6. Noise distribution after putting an additional Kapton flex circuit grounding connection between the support structure and the hybrid. The grounding scheme is (C). The total noise is represented by red squares, and differential noise by light blue circles. The unit is  $\times 10$  ADC counts.

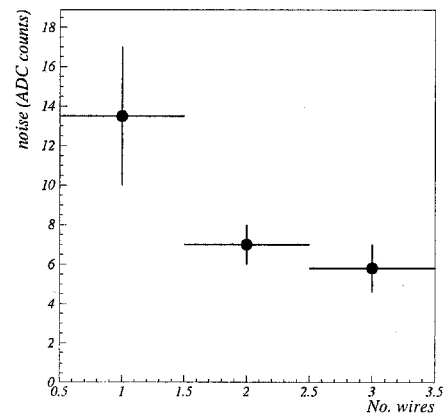


Fig. 7. Noise in terms of ADC counts as a function of number of wires connecting the hybrid ground and the Faraday cage.

## V. PROPOSAL OF GROUNDING SCHEME

### A. General Concept

In principle a single point grounding scheme gives better noise performance than a multi-point one. However, it is difficult to achieve a single point ground for L0 because of the tight space constraints. For example, the support structure of the outer layer of L0 can easily couple to the L0 capacitively, resulting in the breakdown of the single point grounding scheme. Therefore, we chose to implement a multipoint ground, i.e. all hybrids and all sensors will be tied to the ground mesh.

Since the outer layer of the L0 (referred to as L1) also uses carbon fiber as the support structure, we plan to tie both the L0 and L1 structure together. This configuration also provides some additional shielding for L0; it acts like a Faraday cage.

### B. The Local Grounding Scheme

Making low inductance connections to the sensor is straightforward. The Kapton flex with copper mesh is embedded on the surface of the L0 support structure. Another Kapton flex under the sensor provides a grounding path from the HV filter card to the L0 support. The gold plated connection pads on the two Kapton flexes are glued to each other with silver epoxy.

To minimize the inductance due to the area between the analog cable and ground plane, a uniform continuous ground plane between the sensor and hybrid is needed. Since the L0 support and the hybrid support are separate pieces, the inner cylinder is covered with another Kapton flex circuit which is connected to the L0 support structure with a small tab.

Grounding the hybrid is more difficult because there is a ( $>15$  mm for B-sector) space between the hybrid and the well grounded inner cylinder. In addition, there are many parts with complicated geometry which are also made of carbon fiber and must be grounded. Based on the rule of low inductance connections, the shortest path from the hybrid to the inner cylinder was chosen. In addition a wide strip rather than a wire is used.

## VI. CONCLUSION

A low inductance grounding scheme with the smallest possible ground loop is essential to achieve low noise for L0. This implies the use of short and wide electrical connections, and a careful mechanical design to minimize or eliminate any ground loops. Detector designers are usually well aware of these rules, but sometimes forget to apply them or do not realize the importance inductance.

## REFERENCES

- [1] The CDF II Collaboration. "Proposal for Enhancement of the CDF II Detector: An Inner Silicon Layer and A Time of Flight Detector". Fermilab Proposal 909.
- [2] D0 Run 2B Silicon Detector Technical Design Report, Fermilab, Pub-02-327-E.
- [3] Dyconex AG, Grindelstrasse 40, CH-8303 Bassersdorf, Switzerland

